DOI 10.1007/s11182-019-01620-3

Russian Physics Journal, Vol. 61, No. 10, February, 2019 (Russian Original No. 10, October, 2018)

SILICA MONOLITH PROPERTIES MODIFIED BY REACTION MIXTURE COMPOSITION AND CALCINATION PROCESS

O. Yu. Vodorezova,[1] I. N. Lapin,[1] G. V. Lyamina,[2] and T. I. Izaak[1] UDC 544.032

The paper presents the sol-gel synthesis of porous silica monolith in the presence of cetyltrimethylammonium bromide and polyethylene glycol. Parameters of the porous structure and mechanical properties of silica monolith are varied by the reaction mixture composition and reprecipitation and thermal treatment conditions. Mechanical properties and permeability of obtained material are investigated and optimal parameters are identified for the synthesis of porous silica monolith for flow reactors.

Keywords: silicon dioxide, porous monolith, catalyst support, mechanical properties, permeability.

INTRODUCTION

Porous monoliths are used in various fields including catalysis, adsorption, chromatography, and mixture separation. Permeability and mechanical properties of porous monoliths are important in flow reactor applications. Moreover, in some cases, materials should possess a large specific surface area.

Among porous monoliths, materials with a hierarchical structure with extended pores of two or more types such as coalescent macro and micropores, possess a spectrum of unique properties. Each of the pore type is characterized by a proper functional load. A great number of nanosized pores provides a large specific surface area, whereas several micrometers-sized pores form channels for gas and liquid transport adding high permeability to material.

Bimodal and trimodal porous structures are obtained by a microphase separation in gels that allows stabilizing transient states during the gelling process [1]. The process of phase separation and template synthesis can be enabled by surfactants or polymers that provide a synthesis of inorganic materials with a pore size distribution featuring both narrow micropores and wide macropores. Smått *et al.* [2] obtained a hierarchical porous silica material using the cationic surfactant cetyltrimethylammonium bromide (CTAB) and the nonionic substance polyethylene glycol (PEG). The porosity of resulting porous materials achieved 90 % and was characterized by a great deal of through pores and, consequently, the lower flow resistance than in sintered materials representing close-packing of equal spheres studied in [3, 4].

However, the achievement of high porosity and permeability is often accompanied by the deterioration of the mechanical properties of material, namely the low crushing strength. Therefore, it is important to study the possibility of combining the mechanical and transport properties of materials having a bimodal and trimodal porous structure because only a few works considered mechanical properties of such materials [5, 6].

High porosity can be achieved through the additional material treatment, after the formation of a highly permeable structure. For example, sintering of a porous silica monolith at high temperatures can lead to sintering of its skeleton and the improvement of mechanical properties.

[1]National Research Tomsk State University, Tomsk, Russia, e-mail: olga.vodorezova@yandex.ru; 201kiop@mail.ru; taina_i@mail.ru; [2]National Research Tomsk Polytechnic University, Tomsk, Russia, e-mail: lyamina@tpu.ru. Translated from Izvestiya Vysshikh Uchebnykh Zavedenii, Fizika, No. 10, pp. 165–171, October, 2018. Original article submitted September 12, 2018.

In this work we study the porous silica monolith prepared by the sol-gel method in the presence of CTAB and PEG. The porous structure and mechanical properties of the silica monolith are examined *via* changes in the reaction mixture composition, reprecipitation and calcination conditions.

EXPERIMENTAL

Preparation of porous silica monoliths

Silica (SiO_2) monolithic samples with the diameter of 7–10 mm were prepared by the sol-gel method proposed in [7]. The structural parameters were changed by varying the PEG content in the reaction mixture, the molar weight of which was 35000. The weight ratio PEG/SiO_2 in the reaction mixture was varied from 0.24 to 0.54. This range was limited by the crack resistance of obtained samples. The required PEG content was dissolved in 10.5 ml of 1 M nitric acid followed by the addition of 7.6 ml of tetraethoxysilane and then 0.4 g of CTAB. This mixture was stirred at room temperature during 1 hour. The obtained sol was then autoclaved at 40°C for 7 days to let the processes of gelling, microphase separation and gel ageing occur. Further treatment of SiO_2 monolithic samples was necessary to SiO_2 partial reprecipitation. Two types of treatment were used. Type A: in an autoclave, in a 1 M aqua ammonia exceeding 10 times the SiO_2 monolith volume, at 90°C for 9 hours; type B: in a 25% aqua ammonia, at 25°C for 7 days. The samples were then dried at room temperature and calcined at 550°C temperature and higher.

Methods

A VEGA3 SB scanning electron microscope (SEM) (TESCAN, Czech Republic) was used for the surface morphology investigations of SiO_2 monolithic samples. At a nanoscale level, the structural properties were analyzed by the nitrogen adsorption isotherm at –196°C obtained on a TriStar II 3020 analyzer (Micromeritics, USA) using Brunauer–Emmett–Teller and Barrett–Joyner–Halenda methods. Prior to these studies, the sample weights were subjected to vacuum degassing at 250°C for 2 hours. The X-ray phase analysis was carried out by a MiniFlex 600 diffractometer (Rigaku, Japan) equipped with a graphite monochromator. The XRD data were measured from 2° to 40° in 2θ Bragg-angle. Measurements were conducted using copper K_α radiation.

The permeability coefficient K (m^2) for the porous silica monolith is obtained from Darcy's equation:

$$\ln\left(\frac{H}{H_0}\right) = -K\left(\frac{\rho \cdot g}{z \cdot \eta}\right)t\,. \qquad (1)$$

The dependence between $\ln(H/H_0)$ and time (t, s) (where H, m is the height of water with ρ (kg/m^3) and viscosity η (Pa·s) at a free water flow under the SiO_2 layer with z thickness) is linear that proves the use of Eq. (1). And the inclination of the line is proportional to the permeability coefficient K [8].

The porosity of the silica monolithic samples is measured by the moisture capacity. The crushing strength measurements are carried out on an IPG-1M (Russia) instrument using the resulting value as an arithmetic mean value obtained in three batch experiments.

A vacuum dilatometer DIL 402 E/7/G-Py (Netzsch, Germany) was used to determine the thermal length changes for sintered silica gel samples. The samples were manipulated in argon gas at a temperature not over 1300°C and a heating rate of 2 degrees-per-minute followed by cooling down to 50°C at a rate of 5 degrees-per-minute. The linear parameters of the reference alundum sample were measured under the same conditions. All these samples were preliminary calcined at 550°C to remove remained organic substances and water which can distort the kinetic curve shape of the material sintering.

TABLE 1. Parameters of Porous Silica Monoliths *vs.* PEG/SiO_2 After 550°C Calcination.

Samples	Porosity ε, %	Permeability coeff. K, m^2	Strength, MPa	Specific surface area S, m^2/g	Mesopore diameter d_m, nm	Mesopore volume V, cm^3/g	Sphere diameter D_s, μm	Pore diameter D_p, μm
A-0.24	91	$1.5\cdot10^{-11}$	0.18	368	3; 20	0.94	10.5	13
A-0.29	90	$9.1\cdot10^{-12}$	0.14	352	3; 15	1.00	7.75	12
A-0.39	90	$1.0\cdot10^{-11}$	0.21	301	3; 20	1.07	6.2	5.5
A-0.42	93	$2.4\cdot10^{-12}$	0.11	553	2.8; 10	1.00	4.5	4.8
A-0.44	92	$1.8\cdot10^{-14}$	0.45	379	3; 20	1.19	–	–
A-0.46	88	$1.4\cdot10^{-15}$	1.2	355	3; 20	1.05	–	–

RESULTS AND DISCUSSION

Structural parameters of SiO_2 samples affected by the mixture composition

The effect from the ratio PEG/SiO_2 on the structure and crushing strength of SiO_2 monoliths obtained at 550°C calcination is studied depending on the PEG content in the reaction mixture composition. These data are gathered in Table 1. Sample indications include the type of reprecipitation and the PEG/SiO_2 mass ratio.

According to Table 1, mesopores are observed in all SiO_2 samples in the amount of about 1 cm^3/g and represent two types, namely 3 nm and 10–20 nm in size which constitute 70% of porosity at 2.36 g/cm^3 density of amorphous silica. Apparently, a 90% total porosity is defined by 50 nm macropores, whose amount cannot be detected by the nitrogen adsorption. When the PEG/SiO_2 mass ratio increases up to 0.39, the specific surface area varies between 368 and 301 m^2/g. Its further increase from 0.42 to 0.46 results in the decrease in the specific surface area from 553 to 355 m^2/g. This tendency of changing the specific surface at varying the PEG/SiO_2 mass ratio coincides with the change in the size of small and large mesopores.

According to the permeability coefficient K, SiO_2 samples can be divided into two groups that indicate the difference in their structure. For high permeable monoliths, the permeability coefficient ranges within 10^{-11}–10^{-12} m^2. The permeability coefficient of low-permeability samples is lower than 10^{-14} m^2. Therefore they are not suitable for the use in the liquid-phase catalysis despite their high crushing strength. Thus, the ratio of PEG/SiO_2 = 0.42 is the upper limit for synthesizing a macroporous SiO_2 monolith with the permeable structure.

As can be seen in Fig. 1, SiO_2 samples with the PEG/SiO_2 ratio not over 0.42 are porous, and their skeleton comprises almost spherical globules with the size ranging from 10.5 to 4.5 μm (Table 1). It is found that with the increasing PEG concentration the size of globules reduces as well as the size of macropores. This is in good agreement with findings obtained in the literature [9]. The decrease in the pore size causes the decrease in the permeability of SiO_2 monoliths. A further growth in the PEG amount results in the formation of the low-permeability monolith structure. In these samples we do not observe macropores larger than 100 nm in size.

Reprecipitation conditions of the obtained gel also exert a significant effect on the structure of the final product. When the concentration of ammonia and, consequently, pH medium grows, SiO_2 solubility also increases and reprecipitation processes occur more intensively. As can be seen in Fig. 1*f*, a complete structure transformation occurs in B-0.39 sample with the formation of globules and pores smaller than in A-0.39 sample treated with 1 M aqua ammonia (Fig. 1*c*). The porosity lowers from 90 to 87%, the total amount of mesopores decreases from 1.07 to 0.17 cm^3/m, and the specific surface area lowers from 301 to 160 m^2/g. The mass transfer occurs between loose- and dense-graded aggregates with the clogging of the latter, that is manifested by the formation of a denser packing, the increase in the skeleton crushing strength up to 1.36 MPa and the decrease in the monolith permeability down to $1.27\cdot10^{-14}$ m^2. These changes are explained by the classical mechanism of Ostwald ripening.

Figure 2 depicts the XRD pattern typical for all porous silica monoliths. SiO_2 represents the amorphous phase, and the reflection at $2\theta < 2°$ indicates to the formation of ordered 3 nm mesopores with the CTAB involvement [10].

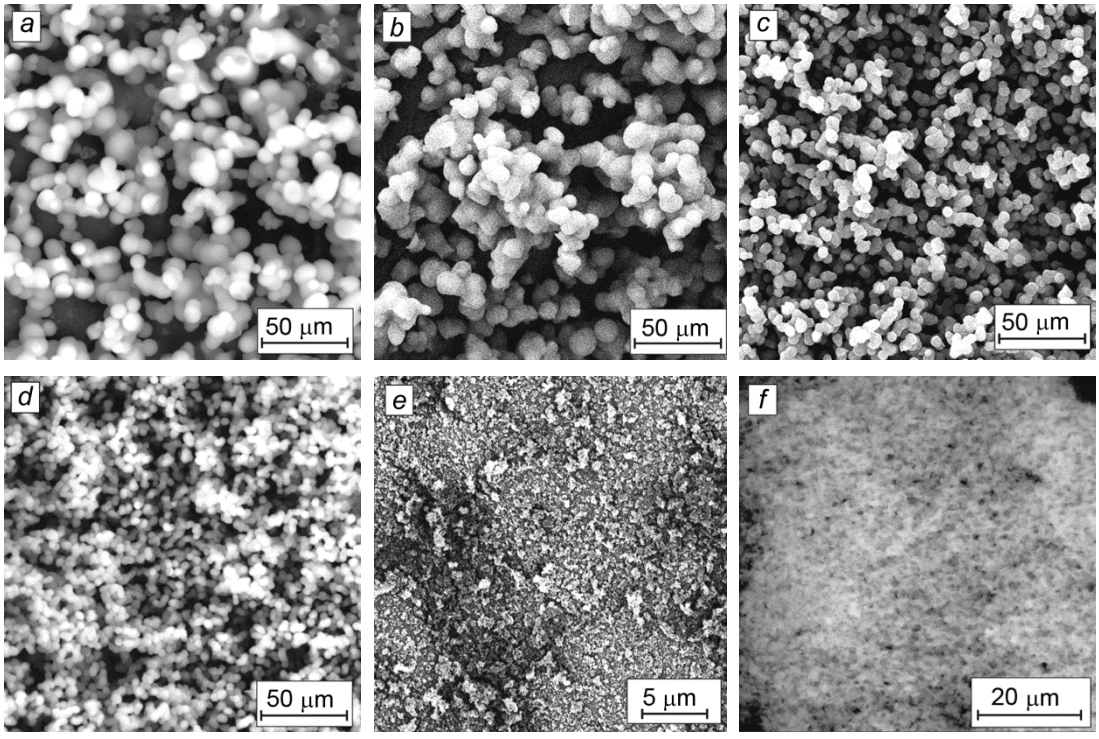

Fig. 1. SEM images of porous silica monoliths obtained after 550°C calcination: A-0.24 (*a*), A-0.29 (*b*), A-0.39 (*c*), A-0.42 (*d*), A-0.44 (*e*), B-0.39 (*f*).

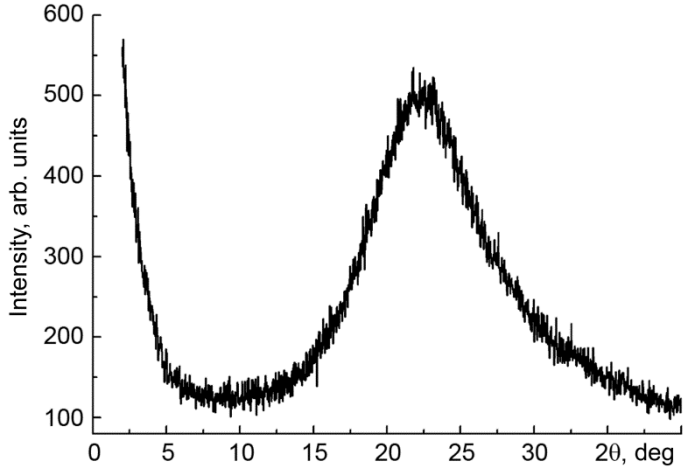

Fig. 2. XRD pattern of A-0.39 sample.

As can be seen from Table 1, the best porosity and permeability of the porous silica monolith are achieved at the ratio of PEG/SiO_2 = 0.39. However, the achieved crushing strength is not enough to apply it in liquid flow reactors and fuel cells.

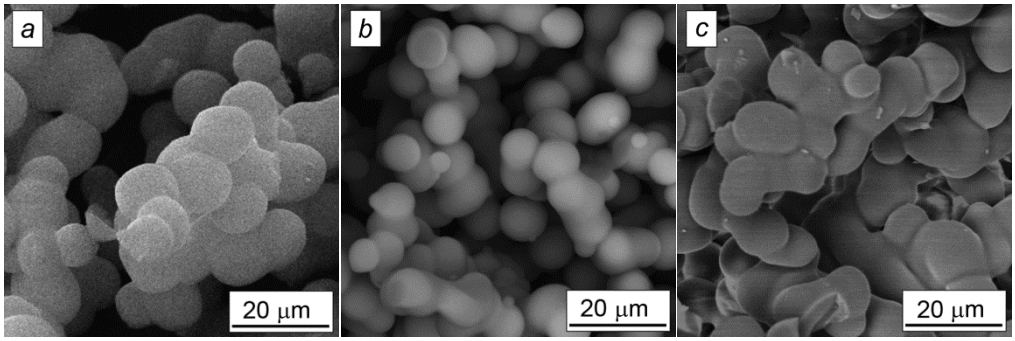

Fig. 3. SEM images of A-0.39 sample at 550°C (*a*), 1000°C (*b*) and 1300°C (*c*) calcination.

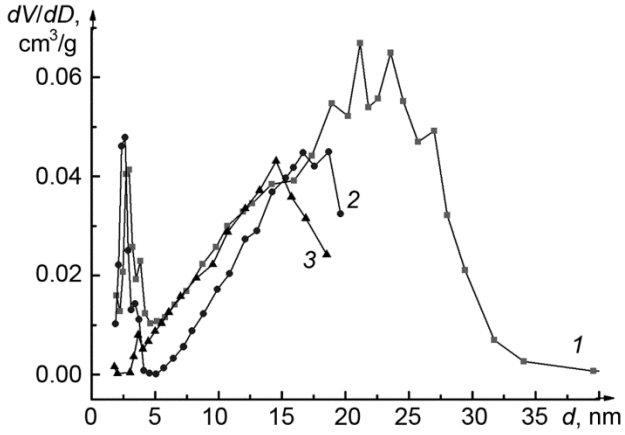

Fig. 4. Pore size distribution in A-0.39 sample at different calcination temperature: *1* – 550°C, *2* – 800°C, *3* – 1000°C.

Thermal treatment effect on SiO_2 sample parameters

The additional method to strengthen SiO_2 samples is sintering. During the thermal treatment of silica gel-based monoliths, dehydration reactions occur between surface silanol groups with the formation of siloxane bridges [11] making the SiO_2 skeleton denser. A packing density of Si–OH groups and high-curvature surface of pores also facilitate these processes. SEM images presented in Fig. 3 show that unlike to 550°C calcination, calcination of A-0.39 sample at 1000°C leads to the decrease in the globule size due to shrinkage and the increase in their contact surface due to sintering. The temperature growth up to 1300°C intensifies the process of sintering, and the boundaries between globules become imperceptible.

According to SEM images, the temperature increase from 550 to 1000°C leads to the insignificant decrease in the porosity and the average size of transport pores. The specific surface area of SiO_2 samples lowers due to the decrease in the pore number. The pore size distribution depending on the calcination temperature is plotted in Fig. 4. It is shown that with the temperature increase the amount of pores reduces, the pore size distribution narrows, and the diffraction peak shifts toward the lower pore size. At 800°C calcination, the size and the amount of large mesopores decrease, whereas the distribution of 3 nm pores narrows. At 1000°C calcination, 3 nm pores disappear (see Table 2).

The dilatometric curve presented in Fig. 5 allows us to assess the sample sintering. As can be seen in this figure, the point contacts appear prior to 570°C calcination (start of sintering), since the sample neither expands nor

TABLE 2. Parameters of A-0.39 Sample *vs.* Calcination.

Temperature, °C	Porosity ε, %	Permeability coeff. K, m^2	Strength, MPa	Specific surface area S, m^2/g*	Mesopore diameter d_m, nm	Mesopore volume V, cm^3/g	Sphere diameter D_s, μm	Pore diameter D_p, μm
550	90	$1.0 \cdot 10^{-11}$	0.21	301	3; 20	1.08	6.2	5.5
800	87	$1.1 \cdot 10^{-11}$	0.41	331	2.7; 17	0.77	4.7	4.7
1000	75	$2.7 \cdot 10^{-11}$	0.55	117	14	0.41	4.6	4.3

* Percentage error: Δ ± 10%.

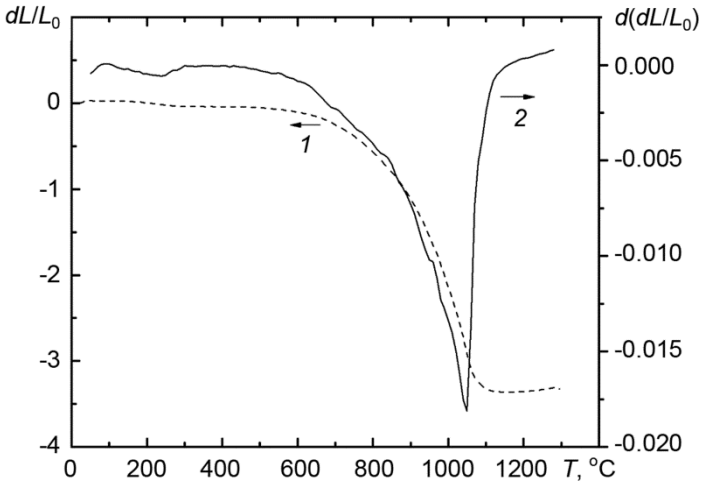

Fig. 5. Integral (*1*) and differential (*2*) curves of A-0.39 sample sintering.

shrinks. A considerable change in the linear size of material occurs at the calcination temperature higher than 600°C that is connected with the decrease in the average size of pores and the skeleton accompanied by the monolith packing and shrinkage. The highest shrinkage rate lies within a 900–1050°C temperature range. The increase in the surface diffusion at higher temperatures facilitates the sintering process.

At 1100–1200°C calcination, the second stage of sintering is observed. The shrinkage rate significantly lowers, but the sample does not yet expand that indicates to the residual porosity in material. Dilatometric tests show that the degree of the sample shrinkage is 45.4% after sintering. The reduction in its length occurs due to the globule sintering which constitute the monolith skeleton. Thus, the globule size reduces from 6.20 to 4.55 μm, *i.e*. by 26%. At the last stage, within a 1200–1300°C temperature range, the sintered sample expands. This is supported by the coefficient of linear thermal expansion equaling $5.3 \cdot 10^{-6}$ 1/K. The coefficient of linear thermal expansion of sintered ceramics usually lies within this temperature range.

CONCLUSIONS

These studies showed that strong and highly permeable, hierarchically structured porous silica monoliths can be produced through the addition of cationic and nonionic surfactants in the reaction mixture composition. The variation of the component ratios allowed controlling the structure, *i.e.* the increase in the PEG/SiO_2 ratio changed the macroscale level parameters, while the introduction of CTAB provided the formation of mesopores. The concentration of PEG and SiO_2 ranged from 0.24 to 0.42, thereby forming the macroporous structure with interconnected macropores.

A change in the reprecipitation mode resulted in a significant structural change of SiO_2 monolith. The porous silica monolith permeability and crushing strength were optimized with the autoclave treatment at 90°C for 9 hours in a 1 M aqua ammonia exceeding 10 times the SiO_2 monolith volume.

Calcination of porous silica monoliths improved their crushing strength without sacrificing high permeability. The porosity and specific surface area of SiO_2 samples tended to decrease owing to the reduction in the amount of non-transport mesopores. The main strengthening effect was observed at the temperature increase up to 800°C, ordered mesopores and the high specific surface area being remained. Therefore, the crushing strength of silica monoliths was improved twice with the same permeability coefficient allowing to synthesize a mechanically strong and high permeability catalyst support for flow reactors and fuel cells.

The authors like to express their gratitude towards the management of Tomsk Regional Core Facility Centre of National Research Tomsk State University for equipment employed in these studies.

REFERENCES

1. K. Nakanishi, Hierarchically Structured Porous Materials: From Nanoscience to Catalysis, Separation, Optics, Energy, and Life Science, Bao-Lian Su, Clément Sanchez, Xiao-Yu Yang, eds., Wiley-VCH Verlag GmbH & Co. KGaA, Weinheim (2012), pp. 241–267.
2. J.-H. Smått, S. Schunk, and M. Linde´n, Chem. Mater., **15,** 2354–2361 (2003).
3. P. Colombo, C. Vakifahmetoglu, and S. J. Costacurta, Mater Sci., **45**, 5425–5455 (2010).
4. M. D. M. Innocentini, P. Sepulveda, V. R. Salvini, *et al.*, J. Am. Ceram. Soc., **81,** No. 12**,** 3349–3352 (1998).
5. R. Takahashi, S. Sato, T. Sodesawa, *et al.*, Mater. Res. Bull., **40**, 1148–1156 (2005).
6. R. Takahashi, S. Sato, T. Sodesawa, *et al.*, Mater. Res. Bull., **42,** 523–531 (2007).
7. A. Koreniuk, K. Maresz, K. Odrozek, *et al.*, Appl. Catal. A, **489**, 203–208 (2015).
8. K. Szymańska, K. Odrozek, A. Zniszczoł, *et al.*, Chem. Eng. J., **315**, 18–24 (2017).
9. T. Hara, G. Desmet, G. V. Baron, *et al.*, J. Chromatogr. A, **1442**, 42–52 (2016).
10. J. Babin, J. Iapichella, B. Lefèvre, *et al.*, New J. Chem., **31**, 1907–1917 (2007).
11. P. Liu, Q. Wang, X. Li, and C. Zhang, Colloids and Surf. A: Physicochem. Eng. Aspects, **334**, 112–115 (2009).